Annals of Botany **112**: 1223–1238, 2013
doi:10.1093/aob/mct206, available online at www.aob.oxfordjournals.org

ANNALS OF BOTANY
Founded 1887

RESEARCH IN CONTEXT

A unifying conceptual model for the environmental responses of isoprene emissions from plants

Catherine Morfopoulos[1,*], Iain C. Prentice[2,3], Trevor F. Keenan[3], Pierre Friedlingstein[4], Belinda E. Medlyn[3], Josep Peñuelas[5,6] and Malcolm Possell[7]

[1]*Department of Life Sciences, Imperial College, Silwood Park, Ascot SL5 7PY, UK,* [2]*AXA Chair of Biosphere and Climate Impacts, Department of Life Sciences and Grantham Institute for Climate Change, Imperial College, Silwood Park, Ascot SL5 7PY, UK,* [3]*Department of Biological Sciences, Macquarie University, Sydney, NSW 2109, Australia,* [4]*College of Engineering, Mathematics and Physical Sciences, Streatham Campus, University of Exeter, Exeter, EX4 4QF, UK,* [5]*CREAF, Cerdanyola del Vallés E-,08193, Barcelona, Spain,* [6]*CSIC, Global Ecology Unit CREAF-CEAB-UAB, Cerdanyola del Vallés, 08193, Barcelona, Spain and* [7]*Faculty of Agriculture and Environment, The University of Sydney, Sydney, NSW 2006, Australia*
** For correspondence. E-mail c.morfopoulos@imperial.ac.uk*

Received: 27 March 2013 Returned for revision: 7 May 2013 Accepted: 9 July 2013 Published electronically: 19 September 2013

• *Background and Aims* Isoprene is the most important volatile organic compound emitted by land plants in terms of abundance and environmental effects. Controls on isoprene emission rates include light, temperature, water supply and CO_2 concentration. A need to quantify these controls has long been recognized. There are already models that give realistic results, but they are complex, highly empirical and require separate responses to different drivers. This study sets out to find a simpler, unifying principle.
• *Methods* A simple model is presented based on the idea of balancing demands for reducing power (derived from photosynthetic electron transport) in primary metabolism versus the secondary pathway that leads to the synthesis of isoprene. This model's ability to account for key features in a variety of experimental data sets is assessed.
• *Key results* The model simultaneously predicts the fundamental responses observed in short-term experiments, namely: (1) the decoupling between carbon assimilation and isoprene emission; (2) a continued increase in isoprene emission with photosynthetically active radiation (PAR) at high PAR, after carbon assimilation has saturated; (3) a maximum of isoprene emission at low internal CO_2 concentration (c_i) and an asymptotic decline thereafter with increasing c_i; (4) maintenance of high isoprene emissions when carbon assimilation is restricted by drought; and (5) a temperature optimum higher than that of photosynthesis, but lower than that of isoprene synthase activity.
• *Conclusions* A simple model was used to test the hypothesis that reducing power available to the synthesis pathway for isoprene varies according to the extent to which the needs of carbon assimilation are satisfied. Despite its simplicity the model explains much in terms of the observed response of isoprene to external drivers as well as the observed decoupling between carbon assimilation and isoprene emission. The concept has the potential to improve global-scale modelling of vegetation isoprene emission.

Key words: Isoprene, modelling, electron transport, photosynthesis, temperature, carbon dioxide, isoprene emission, volatile organic compounds.

INTRODUCTION

Isoprene (2-methyl-1,3-butadiene; C_5H_8) is a highly volatile and reactive unsaturated hydrocarbon that is produced continuously in daylight by many terrestrial plants, and in great abundance by broadleaved trees. On a mass basis, it is the most important biogenic volatile organic compound (BVOC) emitted by vegetation, with an annual global emission of approximately $0{\cdot}5 \times 10^{15}$ g C. This is similar in magnitude to the total annual emission of the greenhouse gas methane (CH_4) from all natural sources combined (Guenther *et al.*, 1995, 2006; Laothawornkitkul *et al.*, 2009). Although not a greenhouse gas itself, isoprene reacts in the atmosphere with oxidants, including hydroxyl radicals (OH) and ozone (O_3) (Fan and Zhang, 2004), and consequently influences the atmospheric lifetime and concentration of CH_4 (Poisson *et al.*, 2000; Collins *et al.*, 2002, 2010; Pike and Young, 2009). The influence of isoprene on atmospheric oxidation capacity has been proposed as one of the controls of the glacial–interglacial variations of atmospheric CH_4, as recorded in ice cores (Valdes *et al.*, 2005; Singarayer *et al.*, 2011). Isoprene also enhances the production of tropospheric ozone (O_3), a potent greenhouse gas and toxic pollutant, under high-NO_x conditions (Sanderson *et al.*, 2003; Hauglustaine *et al.*, 2005), and can significantly affect the atmosphere's radiative balance through the generation of secondary organic aerosols (Claeys *et al.*, 2004; Heald *et al.*, 2008; Carlton *et al.*, 2009; Nozière *et al.*, 2011).

Isoprene emissions by plants at the leaf scale respond to changes in photosynthetically active radiation (PAR), temperature, ambient CO_2 concentration and drought (Sharkey and Yeh, 2001; Laothawornkitkul *et al.*, 2009; Pacifico *et al.*, 2009; Niinemets, 2010). Despite general agreement between

models under the present climate, simulations of future isoprene emissions, and their potential impact on atmospheric chemistry, change dramatically depending on the temperature and light responses of the model (Keenan *et al.*, 2009) and whether the model includes a physiological response of isoprene emission to CO_2 (Heald *et al.*, 2009; Young *et al.*, 2009; Pacifico *et al.*, 2012). Given the continuously increasing atmospheric CO_2 concentration and its impact on future temperature, we need to understand the processes behind observed responses, and use that understanding to build better models.

The adaptive significance of isoprene emission is thought to be connected with enhancing membrane stability at high temperatures, and protection against oxidative stress – including that induced by high temperatures (Sharkey and Yeh, 2001; Vickers *et al.*, 2009; Velikova *et al.*, 2011, 2012). On time scales of weeks to years, acclimation mechanisms acting at the level of gene transcription may operate, possibly in such a way as to match isoprene synthase activity to adaptive requirements (Grote and Niinemets, 2008; Monson *et al.*, 2012; Harrison *et al.*, 2013). Here, however, we focus on the immediate responses of isoprene emission to environmental variations, as observed in experiments conducted over a time scale of minutes to hours, and the basic metabolic mechanisms that may be responsible for them.

The biosynthesis of isoprene occurs via the chloroplastic methylerythritol 4-phosphate (MEP) pathway (Lichtenthaler, 1999; Logan *et al.*, 2000; Sharkey *et al.*, 2008). ^{13}C labelling experiments have shown that the majority of the C in isoprene comes directly from photosynthesis, with the remainder coming from cytosolic C pools depending upon the environmental conditions (Delwiche and Sharkey, 1993; Kreuzwieser *et al.*, 2002; Karl *et al.*, 2002; Affek and Yakir, 2003; Loreto *et al.*, 2004). However, the metabolic controls of the MEP pathway are only beginning to be elucidated (Li and Sharkey, 2012). With incomplete understanding of the metabolic controls of the pathway, models have been developed on the basis of experimental studies of the relationships between isoprene emission and environmental variables. The approach with the longest pedigree combines empirically derived functions for each environmental effect: this is the principle of the MEGAN model (Guenther *et al.*, 2006), developed from the pioneer work of Guenther *et al.* (1993). Other approaches have made more direct use of the limited available information at the biochemical process level, e.g. SIM-BIM (Zimmer *et al.*, 2000, 2003) and the models of Niinemets *et al.* (1999) and Martin *et al.* (2000). Aside from the model from Martin *et al.* (2000), which has an ATP limitation for isoprene production at high internal CO_2 concentration (c_i), all these models need an empirical parameterization to reproduce the observed CO_2 response. This is potentially quite a severe limitation because there may be unforeseen interactions between the effects of different environmental drivers. Empirical models such as MEGAN include a multiplicity of functions for each environmental response of isoprene emission. More mechanistic approaches such as SIM-BIM, on the other hand, require information on many parameters. This might also be an issue because there is a generally accepted trade-off between the multiplicity of required parameter values and model robustness. We set out to identify a unifying principle that might transcend these limitations.

Our starting point was the model of Niinemets *et al.* (1999), which is based on quantifying the NADPH requirement of isoprene synthesis. Niinemets *et al.* (1999) assumed that a certain fraction of the total electron flux generated by Photosystem II is allocated to this function. The model we present here, initially proposed in Harrison *et al.* (2013), builds on Niinemets' work but differs in one fundamental respect: it links isoprene emission to the electron availability for isoprene emission, relative to the needs of CO_2 assimilation. Therefore, the model predicts higher isoprene emissions when absorbed radiant energy (leading to the 'supply' of NADPH) exceeds the 'demand' for CO_2 assimilation. An excess of energy arises because of a mismatch between light availability and carboxylation capacity, which typically occurs daily – especially at high PAR, associated high temperature and under water stress. We compare the model's predictions of observed, published environmental responses of isoprene emission to changes in PAR and the leaf-internal concentration of CO_2 (c_i) with those obtained with the Guenther *et al.* (1993) algorithm, hereafter called G93, which is the basis of the widely used MEGAN model (Guenther *et al.*, 2006), and with the model of Niinemets *et al.* (1999), hereafter called the Niinemets model. We also compare the theoretical temperature responses of our model with G93 and the Niinemets model. We focus on these two models as they have been widely used at the global scale (Guenther *et al.*, 2006; Lathière *et al.*, 2010; Arneth *et al.*, 2011; Pacifico *et al.*, 2012). However, other isoprene models have been developed. Reviews can be found in Arneth *et al.* (2007*a*), Grote and Niinemets (2008), and Monson *et al.* (2012).

HYPOTHESIS

In isoprene-emitting plants with the C_3 pathway of photosynthesis, over 90 % of isoprene production takes place in the chloroplast via the MEP pathway (Lichtenthaler *et al.*, 1997; Sharkey *et al.*, 2008). The final stage is the enzymatic synthesis of isoprene from its precursor, dimethylallyl diphosphate (DMADP). On a per-molecule basis, isoprene synthesis is energetically expensive, and has a high requirement for reducing power (14 NADPH for one molecule of isoprene). For comparison, only six NADPH are needed to synthesize glyceradehyde 3-phosphate (G3P), and only five for pyruvate. NADPH consumption for G3P and pyruvate synthesis takes place within the Calvin cycle and therefore is linked to the electron cost for carbon assimilation. Three additional reducing steps are needed within the MEP pathway to reduce G3P and pyruvate to DMADP. These supplementary reducing steps consume one further NADPH, and two additional reducing equivalents in the form of either NADPH or ferredoxin (Fd) (Charon *et al.*, 1999; Hecht *et al.*, 2001; Seemann *et al.*, 2006; Li and Sharkey, 2012). Our hypothesis focuses on these additional reduction steps, which are directly linked to the production of isoprene.

Isoprene production is typically measured in nanomoles per second while photosynthesis and respiration rates (to which G3P and pyruvate production are linked) are measured in micromoles per second. Hence, the major consumption of reducing power takes place within the Calvin cycle and associated photorespiration while the diversion of reducing power to the MEP pathway is very small. Yet there is abundant circumstantial evidence for a link between the availability of reducing power (after the requirements of carbon assimilation have been accounted for) and the magnitude of this diversion. The MEP pathway is tightly

linked to the photosynthetic apparatus, involves light-dependent reactions and takes place in the chloroplast. Higher isoprene emission capacity is encountered under conditions when photoinhibition occurs, including high light intensities, low c_i and high temperatures. Isoprene emissions decrease if plants are fed with nitrate (note that nitrate reduction to ammonia occurs mainly in the cytoplasm and consumes NAPDH) instead of being fed with ammonia directly (Campbell, 1988; Rosenstiel *et al.*, 2004). Li and Sharkey (2012) measured an extremely high level of the intermediate metabolite, methylerythritol cyclodiphosphate (MEcDP), in an N_2 atmosphere, where the carbon assimilation and photorespiration sinks for NADPH are blocked. Thus, it might be that the MEP pathway acts as a 'branch circuit' with the amount of NAPDH allocated to it increasing in proportion to the amount of reducing power to spare from other functions.

Thus, we hypothesize that isoprene emission is regulated in the short term by variations of the DMADP pool size, linked to the excess or deficit of electrons (and so also reducing power) relative to the needs of carbon assimilation. Figure 1 provides a schematic of the processes involved. When the chloroplast is illuminated, light absorbed by the thylakoids generates the electron flux (J_{tot}) that finally reduces $NADP^+$ to NADPH. Most of the NADPH is used in the Calvin cycle for carbon fixation, but the total NADPH thus generated ($\approx$ 0·5 J_{tot}) exceeds the amount consumed in the Calvin Cycle ($\approx$ 0·5 J_{CO2+O2}). When assimilation is light-limited (at high c_i and/or low PAR) there is still some NADPH available for other functions, which include nitrate reduction (Canvin and Atkins, 1974; Niinemets, 2004; Eichelmann *et al.*, 2011) and DMADP synthesis. When assimilation is Rubisco-limited (at low c_i and/or high PAR) this excess of NADPH becomes larger, allowing more NADPH to be used in DMADP synthesis.

This reasoning suggests the following simple model:

$$Iso = \max\{[\mathbf{a}J + \mathbf{b}(J - J_v)], f(c_i), 0\} \quad (1)$$

where *Iso* is the rate of isoprene emission; $f(c_i)$ is a function of internal CO_2 concentration; J is an estimate of the total electron flux, taken to be a non-rectangular hyperbolic function of absorbed PAR and the maximum electron flux J_{max}, following Farquhar *et al.* (1980); J_v is the electron flux required to support Rubisco-limited carbon assimilation; and **a** and **b** are parameters. The electron flux required to support carbon assimilation is derived as follows (from Farquhar *et al.*, 1980):

$$A_j = (J/4)(c_i - \Gamma^*)/(c_i + 2\Gamma^*) \quad (2)$$

where A_j is the gross (light-limited) assimilation rate and Γ^* is the CO_2 compensation point in the absence of dark respiration. Hence

$$J = 4A_j(c_i + 2\Gamma^*)/(c_i - \Gamma^*). \quad (3)$$

When Rubisco limits photosynthesis, then

$$A_v = V_{cmax}(c_i - \Gamma^*)/(c_i + K_m) \quad (4)$$

where A_v is the gross (Rubisco-limited) assimilation rate, V_{cmax} is the Rubisco capacity and $K_m = K_c(1 + [O_2]/K_o)$ where K_c and

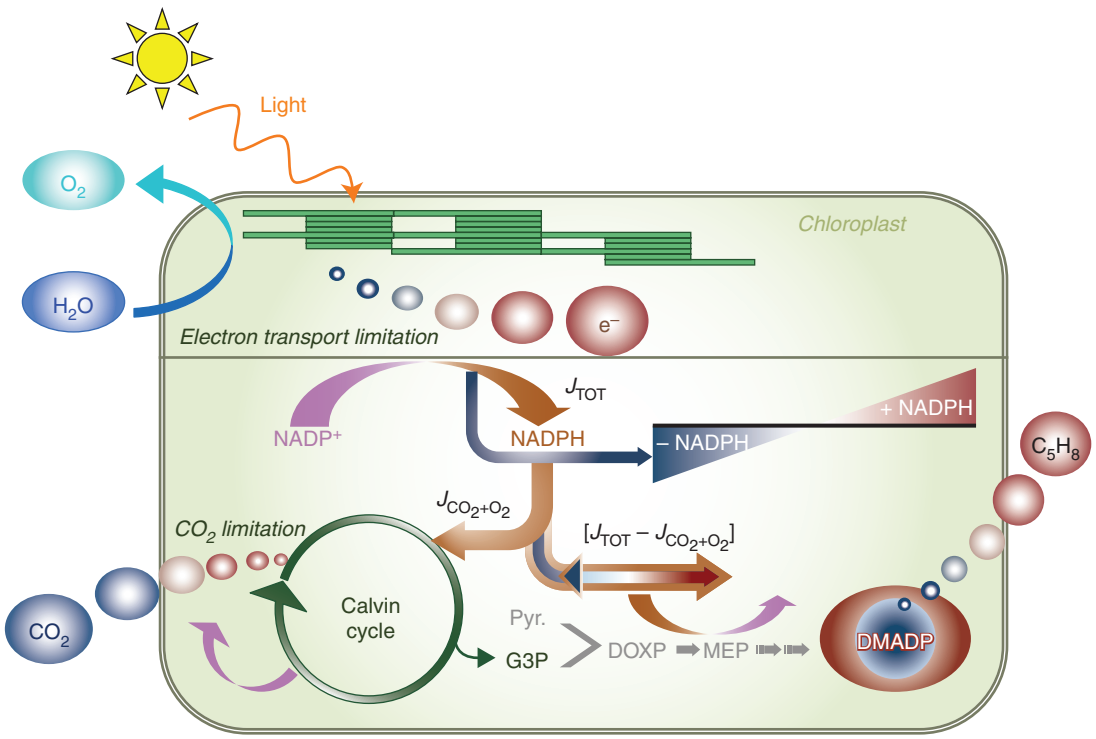

FIG. 1. Schematic of the processes underlying the model of isoprene emissions. The availability of reducing power (NADPH) for CO_2 assimilation is represented by a colour scheme, from dark blue (deficit of NADPH) to dark red (excess of NADPH). Symbols: NADPH and $NADP^+$, nicotinamide adenine dinucleotide phosphate; DMADP, dimethylallyl diphosphate; Pyr, pyruvate; G3P, glyceraldehyde 3-phosphate; DOXP, 1-deoxy-D-xylulose 5-phosphate; MEP, 2-*C*-methyl-D-erythritol 4-phosphate.

K_o are the Michaelis coefficients of Rubisco for CO_2 and O_2 respectively (Farquhar *et al.*, 1980). Substituting this into eqn (3) gives:

$$J_v = 4V_{cmax}(c_i + 2\Gamma^*)/(c_i + K_m). \quad (5)$$

It should be noted that J in eqn (1) is used as an estimate of J_{tot} and could be an underestimate (Singsaas *et al.*, 2001; Niinemets, 2004). More details of the photosynthetic model, as used in this paper, can be found in the Supplementary Data.

The term $\mathbf{a}J$ in eqn (1) represents a 'baseline' of isoprene emission under light-limited conditions under the equilibrium conditions for carbon assimilation ($J = J_v$, energy supply = Rubisco demand), while $\mathbf{b}(J - J_v)$ represents variation in isoprene emission due to the disequilibrium between supply and demand.

The function $f(c_i)$ in eqn (1) is chosen to take the value c_i/Γ^* when $c_i \leq \Gamma^*$ and 1 otherwise. Because of this function, the model differs slightly from the one we proposed in Harrison *et al.* (2013). The function $f(c_i)$ reflects the idea that a minimum rate of supply of carbon chains is required for isoprene synthesis, and the common observation that isoprene emission ceases abruptly when $c_i < \Gamma^*$ (Wolfertz *et al.*, 2003; Rasulov *et al.*, 2009, 2011; Monson *et al.*, 2012; Sun *et al.*, 2012). This fall-off of isoprene at low c_i is not always observed: emission of isoprene in CO_2-free air has been reported in a few studies (Monson and Fall, 1989; Affek and Yakir, 2003; Li and Sharkey, 2012), but comparable conditions are not found in natural environments.

Although based conceptually on the NADPH requirements of isoprene synthesis and the Farquhar photosynthesis model, our approach differs from that of Niinemets *et al.* (1999, 2004) in which isoprene production was assumed to be closely linked to the light-limited carbon assimilation rate (A_j). This difference has important consequences, as we will show.

TESTS OF THE HYPOTHESIS

We consider the observed environmental responses of isoprene emission (*Iso*) and also the ratio of isoprene emission to carbon gross assimilation (Iso/A_{gross}), which is a sensitive indicator of the allocation of reducing power to the MEP pathway versus the Calvin cycle. We will also consider changes in the ratio of isoprene emission to carbon net assimilation (Iso/A_{net}).

Responses to PAR

Equation (1) predicts an increase of isoprene emission with PAR, but also an increase of the ratio Iso/A_{gross} (Fig. 2A). The

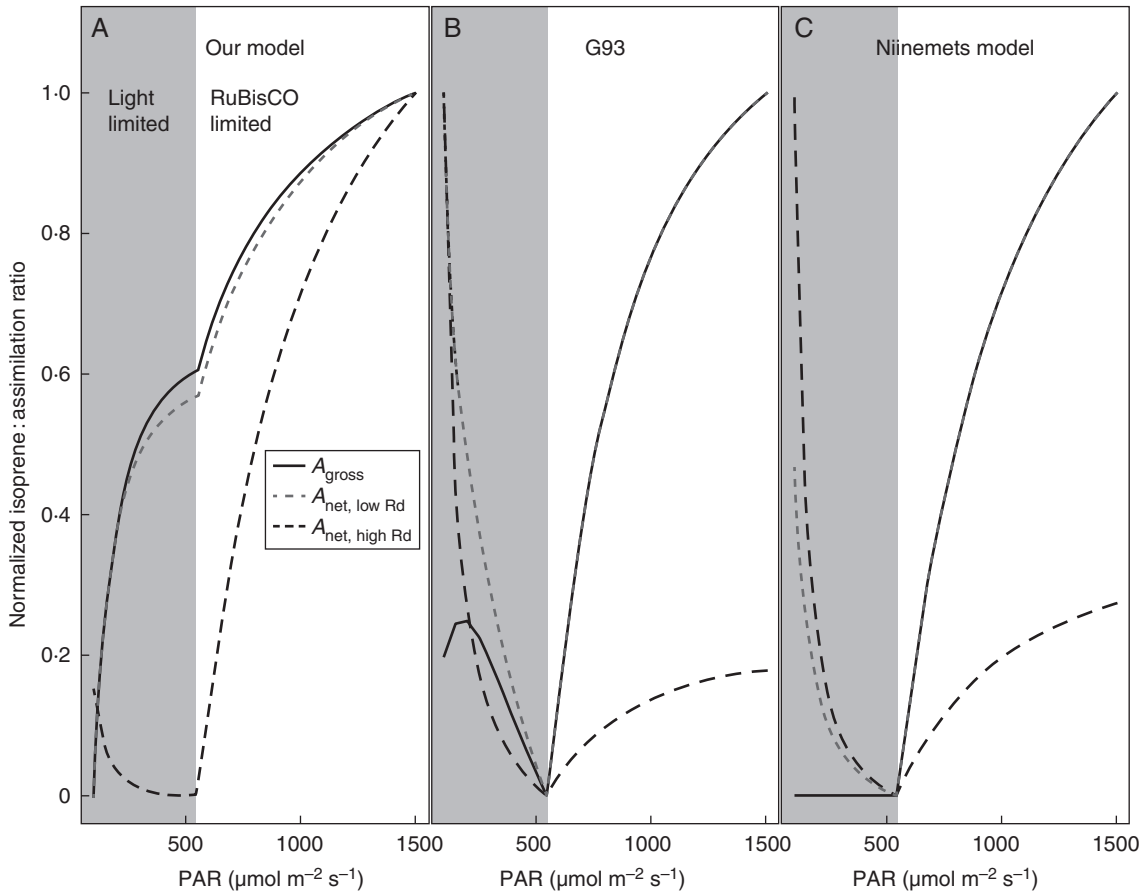

FIG. 2. Modelled responses of the normalized ratio of isoprene to CO_2 assimilation to changes in PAR for (A) our model, (B) G93 and (C) the Niinemets model. $T = 30$ °C, $c_i = 273$ μmol mol^{-1}, $V_{cmax\_25°C} = 70$ μmol m^{-2} s^{-1}, $J_{max\_25°C} = 130$ μmol m^{-2} s^{-1} based on values from Arneth *et al.* (2007*a*). The solid line represents the ratio of isoprene emission to gross assimilation, the dashed line to net assimilation. Normalized ratio of isoprene to CO_2 net assimilation was simulated for two extreme values of dark respiration to illustrate the potential effect of the magnitude of R_d on how Iso/A_{net} varies with PAR: grey short-dashed line, low $R_{d;}$ $R_{d\_25°C}$ = 0·5 μmol m^{-2} s^{-1}; black long-dashed line, high $R_{d;}$ $R_{d\_25°C} = 2$ μmol m^{-2} s^{-1}. Isoprene model parameters **a** and **b** (eqn 1) are based on data of Possell and Hewitt (2011; fig. 6).

predicted behaviour of Iso/A_{net} ($A_{net} = A - R_d$, where R_d is mitochondrial respiration) is substantially different at low PAR, as shown in Fig. 2A. At saturating PAR, the difference becomes less important. This is due to the introduction of the R_d term, which affects the assimilation independently from the allocation of reducing power between carbon fixation and secondary metabolism. Most laboratory experiments have reported only A_{net}; this should be kept in mind while interpreting the results.

The response of normalized Iso/A_{gross} (and Iso/A_{net}) with PAR is predicted to take place in three stages (Fig. 2A).

Stage 1: light-limited carbon assimilation. This stage occurs when PAR absorbed is insufficient to generate an electron flux to satisfy Rubisco capacity. It is characterized by an initial steep increase of Iso/A_{gross} with PAR, becoming gradually less steep at higher PAR. For Iso/A_{net} the form of the response at low PAR depends on the magnitude of R_d.

Stage 2: transition between light- and Rubisco-limited carbon assimilation. This stage is characterized by a discontinuity (abrupt increase) in the slope of Iso/A_{gross} (and Iso/A_{net}) versus PAR.

Stage 3: Rubisco-limited carbon assimilation. When the electron requirement for carbon assimilation is fully satisfied, the additional reducing power generated by increasing PAR allows Iso/A_{gross} to continue increasing while A_{gross} remains constant. In this stage, Iso/A_{net} follows a similar pattern of the Iso/A_{gross} and increases with PAR. With still further increases in PAR, Iso/A_{gross} and Iso/A_{net} eventually saturate, as J tends to its maximal value (J_{max}).

Note that the PAR flux where the transition between light- and Rubisco-limited assimilation occurs (Stage 2) as well as the rate of increase of Iso/A_{gross} with increasing PAR are dependent on both the photosynthetic and the isoprene model parameters.

We also examined the normalized responses of Iso/A_{gross} and Iso/A_{net} to changes in PAR in the G93 and Niinemets models (Fig. 2B, C). Under light-limited conditions (Stage 1), the picture differs dramatically depending on the model. In the Niinemets model, isoprene emissions are tightly linked to A_j (see Supplementary Data) and therefore the response of *Iso* to PAR necessarily has the same shape as that of A_j, irrespective of the chosen values of V_{cmax} or J_{max}. As a result, the ratio Iso/A_{gross} in this model is always constant under light-limited conditions, where carbon assimilation is equal to A_j. The ratio Iso/A_{net}, when simulated with the Niinemets model, always decreases with PAR under light-limited conditions. In G93, by contrast, changes in Iso/A_{gross} with PAR are strongly dependent on V_{cmax}, J_{max} and temperature under light-limited conditions. Consequently, the increase followed by a decrease of Iso/A_{gross} under light-limited conditions, shown in Fig. 2B, is one of the possible responses of Iso/A_{gross} for G93, obtained for the temperature and photosynthetic parameters chosen for this simulation. Changing those parameters changes the shape of the response, and Iso/A_{gross} can decrease or increase at low PAR. Introducing a dark respiration term affects the shape of the response of Iso/A_{net} with PAR, as represented by the dashed lines in Fig. 2B. Hence, G93 can potentially show an Iso/A response to PAR similar to that of our model.

All three models predict increasing Iso/A_{gross} with PAR under Rubisco-limited conditions. Indeed, in the Niinemets model, as isoprene emissions are linked to A_j, they must continue to increase even when carbon assimilation is Rubisco-limited. In that sense, the Niinemets model implicitly allows consumption of extra NADPH above the needs for carbon assimilation (for the PAR response only). For G93, isoprene emission approaches an asymptotic value at high PAR, while the Farquhar model fully saturates under Rubisco-limited conditions at high PAR.

Most studies reporting the fraction of assimilated carbon that is re-emitted as isoprene have found that it increases with PAR, in line with our predictions (Sharkey and Loreto, 1993; Harley *et al.*, 1996; Lerdau and Keller, 1997; Niinemets *et al.*, 2010). However, one study (Lerdau and Throop, 1999) found no significant increase in Iso/A_{net} with PAR for most of the tropical taxa they investigated.

Figure 3A compares the relationships of Iso/A_{net} to PAR in our model and in digitized data from Sharkey and Loreto (1993) on kudzu leaves (*Pueraria lobata*). Assuming J_v is constant (no variation in c_i; Fig. 3B), the observed isoprene emissions show a strong positive linear relationship with J ($r^2 = 0{\cdot}97$). The model parameters **a** and **b** (eqn 1) have been estimated from this linear regression. The Farquhar model parameters were estimated with a best data/model fit by minimizing the residual sum of squares (RSS). The comparison between our model and the data for Iso/A_{net} shows excellent agreement ($r^2 = 0{\cdot}92$). In comparison, G93 and the Niinemets model both show poor agreement ($r^2 = 0{\cdot}19$ and $r^2 = 0{\cdot}06$, respectively). Yet the three models show a good agreement of the modelled isoprene alone (*Iso*) with data (our model: $r^2 = 0{\cdot}97$; G93: $r^2 = 0{\cdot}92$; Niinemets: $r^2 = 0{\cdot}97$; results not shown).

We also compiled data on the response of Iso/A_{net} to PAR from the limited number of published studies to assess the generality of the pattern (Fig. 4). The publications reported A_{net} rather than A_{gross}, and did not typically provide measurements of R_d. As the predicted response of Iso/A_{net} for low PAR is dependent on R_d, it is not surprising to observe an initial decline in Iso/A_{net} with PAR for some of the 18 experiments. More importantly, the great majority of the studies show increasing Iso/A_{net} up to the highest PAR fluxes, especially when photosynthesis saturates (open circles in Fig. 4). In some studies a drop in assimilation rate at high PAR contributed to this increase in Iso/A_{net} at high PAR; this was probably due to stomatal closure at high PAR, resulting in reduced c_i.

As shown in Fig. 2, the Niinemets model cannot reproduce the positive response of Iso/A_{net} to PAR that is generally observed under low PAR. Our model, along with G93, fully captures the shape of the observed response of Iso/A_{net} to PAR over the full range of PAR. But our model also provides a process-based explanation for this response.

We also examined the relationship between Iso/A_{gross} and PAR at the canopy scale, at which isoprene emission is more likely to be controlled by the DMADP pool size than by isoprene synthase activity (Vickers *et al.*, 2010). We used simultaneous CO_2 and isoprene flux measurements made at Harvard Forest, Massachusetts, USA (42·54°N, 72·17°W) (Urbanski *et al.*, 2007; McKinney *et al.*, 2011). Data used were obtained during the 2007 growing seasons using eddy covariance, with proton transfer reaction mass spectrometry used to measure the isoprene mixing ratio (McKinney *et al.*, 2011). Daytime data were selected for temperatures above 23 °C where variations in isoprene emission were no longer significantly driven by

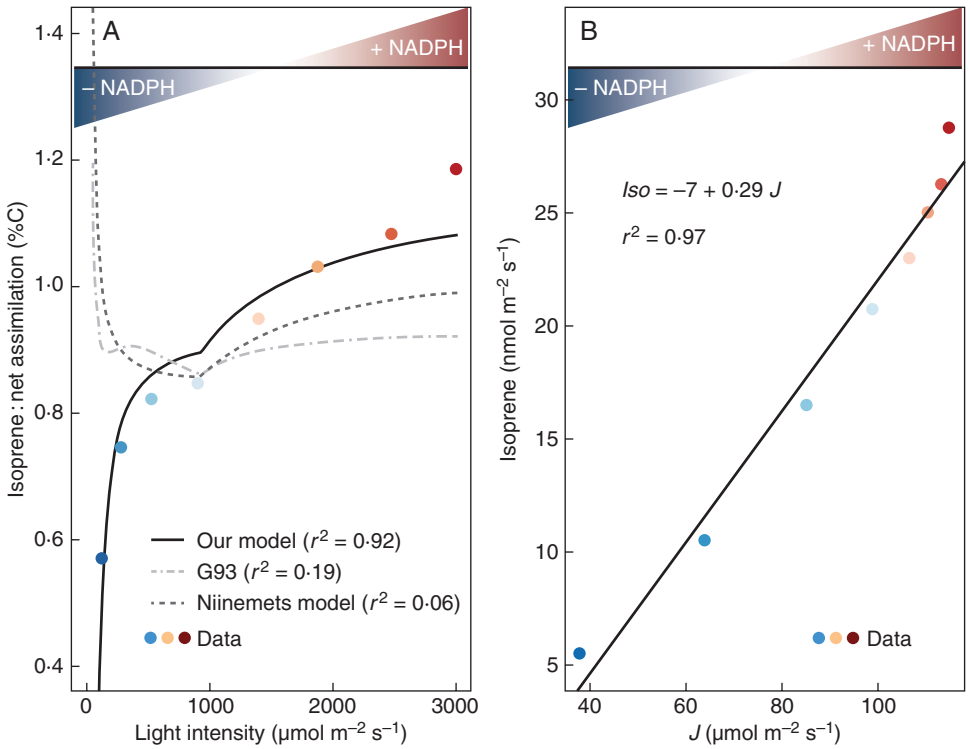

FIG. 3. The relationship between isoprene emission and NADPH availability for carbon assimilation with changing PAR. (A) Increasing values of the isoprene to CO_2 net assimilation ratio with increasing PAR, based on data digitized from figure 2 in Sharkey and Loreto (1993). Simulations made with our model, G93, and the Niinemets model are as indicated in the key. (B) The linear regression between isoprene data and the light-limited electron flux (J). Plant-specific isoprene parameters (**a**, **b**) are estimated from this linear regression and parameters for assimilation (V_{cmax}, J_{max}) were fitted to the assimilation observations by minimizing the residual sum of squares (RSS). In both panels, the availability of reducing power (NADPH) for CO_2 assimilation is illustrated by a colour scheme, from dark blue (deficit) to dark red (excess).

temperature (Fig. A1). Ecosystem respiration, estimated from night-time CO_2 flux measurements, was used to convert the daytime measured net ecosystem CO_2 exchanges into canopy-scale gross assimilation rates. Canopy-scale carbon assimilation shows a typical rectangular hyperbolic response to PAR, but the response of isoprene emission to PAR is closer to linearity, and emissions do not saturate at high PAR (Fig. 5A, B). Thus, above a PAR threshold of approx. 300 μmol m^{-2} s^{-1}, Iso/A_{gross} increases with PAR even at high PAR, where assimilation is light-saturated, consistently with our hypothesis.

Scaling from leaf to canopy involves additional processes, such as within-canopy chemistry and canopy structure effects (Grote, 2007; Keenan *et al.*, 2011; Bryan *et al.*, 2012). Therefore, a canopy model is needed to fully account for these results, especially for low PAR where deposition processes can influence the observed above-canopy isoprene emissions and possibly explain the observed drop in Iso/A_{gross}. Nevertheless these results, along with those of laboratory experiments, corroborate the notion that isoprene emission is related to the availability of electrons generated in photosynthesis, relative to the demand for them to be used in carbon assimilation.

Responses to c_i

Responses of isoprene emission to ambient CO_2 concentration have been widely reported. Plants grown at high atmospheric CO_2 concentrations generally emit less isoprene than those grown at lower CO_2 concentrations. On short time scales, isoprene emission has also been shown to respond strongly and rapidly to c_i, with lower emission rates at higher c_i (Rosenstiel *et al.*, 2003; Wilkinson *et al.*, 2009; Possell and Hewitt, 2011; Sun *et al.*, 2012). The fact that rapid changes in c_i evoke instantaneous responses in isoprene emission suggests that the driving mechanism must be tightly linked to processes in the chloroplast.

The mechanisms behind the decoupling between isoprene emission and carbon assimilation in the response to c_i are not well established. Niinemets *et al.* (1999) hypothesized that the dependency of isoprene emission on c_i might be due to the partitioning of reducing power and ATP into the MEP pathway. However, the model of Niinemets *et al.* (1999) does not allow for any greater partitioning of reducing power to the MEP pathway at low c_i. Isotopic labelling studies have provided evidence for the existence of extra-chloroplastic sources of carbon to support isoprene production. Hence, competition for phosphoenolpyruvate (PEP) between cytosolic and chloroplastic processes has been proposed as an explanation for the drop in isoprene emission at high c_i due to the CO_2-dependence of PEP carboxylase activity (Karl *et al.*, 2002; Rosenstiel *et al.*, 2003; Possell and Hewitt, 2011; Trowbridge *et al.*, 2012). But these experiments compared plants grown at different CO_2 concentrations. Gene expression involving changes in enzyme quantities cannot explain the observed fast (about 10-min) responses to changes in c_i. We focus here only on the short-term responses to c_i, in which isoprene emission appears to be tightly coupled to

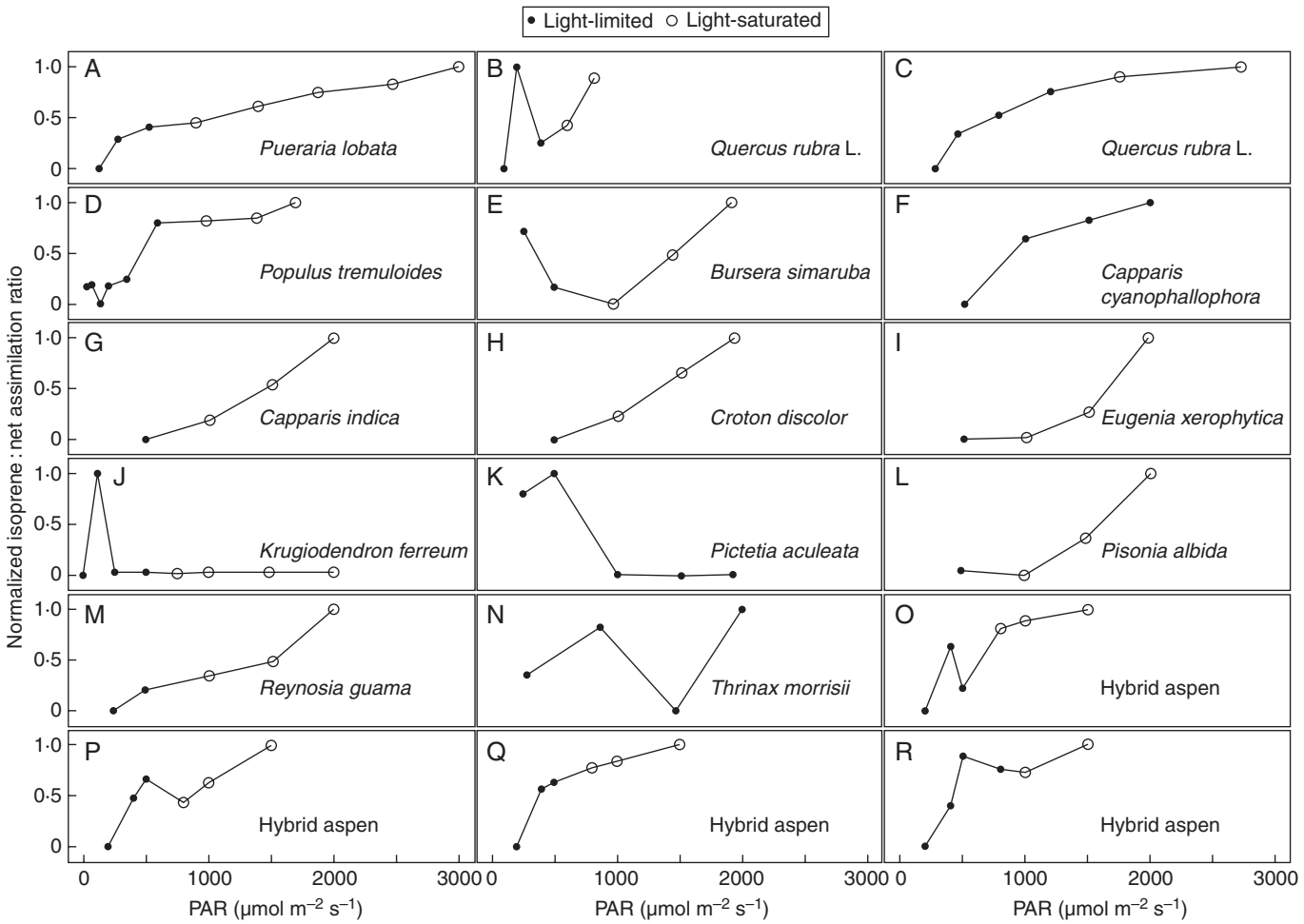

FIG. 4. Observed responses of the normalized ratio (isoprene emission/net CO_2 assimilation) to changes in PAR. Light-limited and light-saturated carbon assimilation as indicated in the key. Data digitized from (A) Sharkey and Loreto (1993), (B, C) Loreto and Sharkey (1990), (D) Monson and Fall (1989), (E–N) Lerdau and Keller (1997), (O–R) Sun *et al.* (2012). (O) Plant grown at ambient CO_2, chamber $[CO_2] = 380$ μmol mol^{-1}. (P) Plant grown at ambient CO_2, chamber $[CO_2] = 780$ μmol mol^{-1}. (Q) Plant grown at elevated CO_2, chamber $[CO_2] = 380$ μmol mol^{-1}. (R) Plant grown at elevated CO_2, chamber $[CO_2] = 780$ μmol mol^{-1}.

changes in the pool size of DMADP (Rasulov *et al.*, 2009). Specifically, we examine whether the fast responses of isoprene emission to c_i could be explained in a simple way by our model, based on the same mechanisms we have proposed to explain the response to PAR.

At low c_i, carbon fixation is Rubisco-limited, resulting in an excess of NADPH (Figs 1 and 6A). The excess of NADPH can be smaller or larger depending on PAR. This provides a simple explanation for why isoprene responses to changes in c_i are light-dependent (Loreto and Sharkey, 1993; Fig. 7D). Moreover, our model can indeed reproduce the isoprene emission response to changes in c_i. This is shown in Fig. 6A using data on *Acacia nigrescens* from Possell and Hewitt (2011). Here, isoprene emission shows a strong negative linear relationship with the Rubisco-limited electron flux, J_v ($r^2 = 0{\cdot}70$), as shown in Fig. 6B. The parameters **a** and **b** (eqn 1) of our model were estimated from this linear regression. When plotted against c_i, our model shows a good agreement with the data ($r^2 = 0{\cdot}70$). Figure 6A also shows the response of the G93 and the Niinemets model with and without a CO_2 inhibition effect (Arneth *et al.*, 2007*a*; Pacifico *et al.*, 2011). It is clear from Fig. 6A that these models do not reproduce the observed response of isoprene emission to c_i. Without an additional empirical function for CO_2 inhibition, isoprene emissions simulated with the Niinemets model are quite out of range. Instead, the model shows a strong negative correlation with the data ($r^2 = 0{\cdot}7$). The negative relationship can be explained by the fact that although the PAR and therefore the light-limited electron flux (J) are constant, light-limited assimilation (A_j) is strongly c_i-dependent. Adding an empirical function to represent the CO_2 inhibition effect, as in Arneth *et al.* (2007*a*), changes the shape of the response (allowing a decrease at high c_i) but still the simulated emissions agree poorly with the data.

Again using the data from Possell and Hewitt (2011), we plotted Iso/A_{net} versus c_i (Fig. 7A) and $J - J_v$ (Fig. 7B). These plots confirm that the fraction of assimilated carbon allocated to isoprene production increases under conditions of NADPH excess. This provides a simple explanation for the response of isoprene emission to c_i. The extremely steep rise in Iso/A_{net} when $J - J_v$ becomes positive is due to the combination of steeply increasing isoprene emission with decreasing assimilation rate as c_i declines.

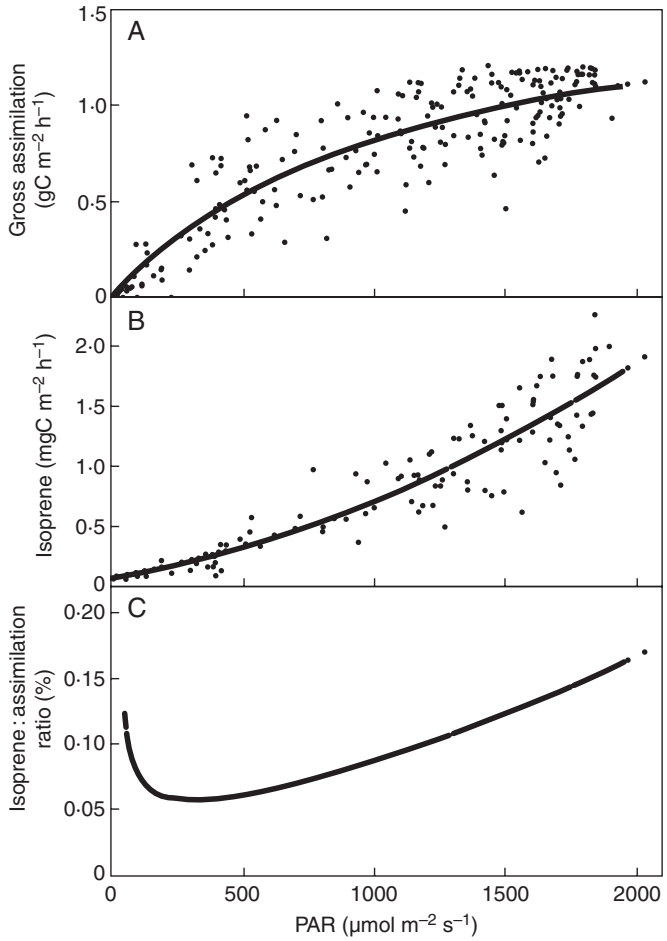

FIG. 5. Above-canopy gross assimilation (A), isoprene emissions (B) and isoprene emission/gross assimilation (C), in relation to PAR. From flux measurements at Harvard Forest.

Loreto and Sharkey (1990) measured changes in isoprene emission with changing c_i at different PAR fluxes in *Quercus rubra*. Both *Iso*/A_{net} and isoprene emission are shown (Fig. 7C, D) to increase with PAR, consistent with a dependence on NADPH availability, at all values of c_i. We compared the responses of G93 and the Niinemets model to c_i at different PAR fluxes, together with our model (Fig. 8). Note that both G93 and the Niinemets model are applied here in their original formulations (see Supplementary Data for details), and therefore do not include additional parameterizations of the CO_2 effect. A number of studies have used these same models with additional empirical functions, introduced specifically to account for the observed CO_2 inhibition (Arneth *et al.*, 2007*b*; Heald *et al.*, 2009; Pacifico *et al.*, 2011). G93 in its original formulation simulates no change at all in isoprene emission with changes in c_i, although it has isoprene emission depending on PAR (Fig. 8B). The Niinemets model in its original formulation also simulates increasing isoprene emission with PAR, but here the modelled emissions *increase* with increasing c_i, due to the fact that this model tightly links isoprene emission to light-limited assimilation (Fig. 8C). Thus, additional functions are required in both models to account for the observed effects of varying c_i. In contrast, our model (Fig. 8A) can reproduce the form of the c_i response shown in the data (Fig. 7D), as well as the effects of combined changes in c_i and PAR (Fig. 7D), without the need for any additional function.

Responses to leaf temperature

The temperature dependence of isoprene emission differs from that of photosynthesis. Temperature optima for carbon assimilation are usually $\leq 30\ ^\circ C$ in C_3 plants, while isoprene emission peaks at $\approx 40\ ^\circ C$ (Guenther *et al.*, 1993; Niinemets *et al.*, 1999; Sharkey and Yeh, 2001; Pacifico *et al.*, 2009). An increase of *Iso*/*A* with temperature is usually observed (Sharkey and Loreto, 1993; Harley *et al.*, 1996; Sharkey *et al.*, 1996; Niinemets *et al.*, 1999; Sharkey and Yeh, 2001). The optimum for isoprene emissions rarely exceeds 40 °C, so the temperature dependence of isoprene emission cannot be fully explained by the temperature dependence of isoprene synthase, which is maximally active between 45 and 48 °C (Monson *et al.*, 1992; Lehning *et al.*, 1999; Niinemets *et al.*, 1999; Rasulov *et al.*, 2010). The decrease in isoprene emissions above 40 °C has long been considered to be linked to the behaviour of the photosynthetic electron transport rate (Guenther *et al.*, 1991; Niinemets *et al.*, 1999). Rasulov *et al.* (2010) found that this decrease is associated with decline in the DMADP pool size and the energetic status of the leaf.

In G93 the temperature dependency of isoprene emission is fixed with a temperature optimum around 38 °C. In the Niinemets model it is assumed to be primarily controlled by IspS activity, with the fraction of electrons used for isoprene production exponentially increasing with temperature. The temperature optimum for isoprene emissions in the Niinemets model is thus close to the optimum for IspS. Some global-scale studies have set an upper limit for the increase of ε with temperature, thereby reducing the temperature optimum to a value closer to 38 °C (Pacifico *et al.*, 2011) (Supplementary Data A.2).

Our model is based on the hypothesis that the production of DMADP depends on photosynthetic electron flux and variations in electron availability for functions other than carbon assimilation. Thus, our modelled optima for isoprene emissions are primarily driven by the behaviour of the light-limited electron flux. Figures 9 and 10 illustrate how a temperature response arises in our model. Carbon assimilation follows the lower of the temperature response curves of the Rubisco and light-limited assimilation rates. Rubisco activity usually has a higher temperature optimum than electron transport (Crafts-Brandner and Salvucci, 2000; Medlyn *et al.*, 2002; Cen and Sage, 2005; Kattge and Knorr, 2007). At high PAR an excess of NADPH can arise for temperatures below the optimum for electron transport (J), so isoprene emissions increase. Above this optimum (T_{opt_J}), J_v still increases even if assimilation is reduced, due to the higher affinity of Rubisco for O_2 at high temperatures. Both J and $(J - J_v)$ decrease for temperatures higher than T_{opt_J} (as illustrated in Fig. 9B). Our model thereby predicts a temperature optimum of isoprene emissions that is closer to the temperature optimum of the electron transport rate. Beyond this optimum, our model predicts a drop in the availability of reducing power, leading to a decrease of DMADP and consequently isoprene emissions. At low PAR (light-limited condition), however, $(J - J_v)$ decreases with increasing temperature, compensating for the increase of J. Predicted emissions are thus almost insensitive to temperature or even decrease with temperature

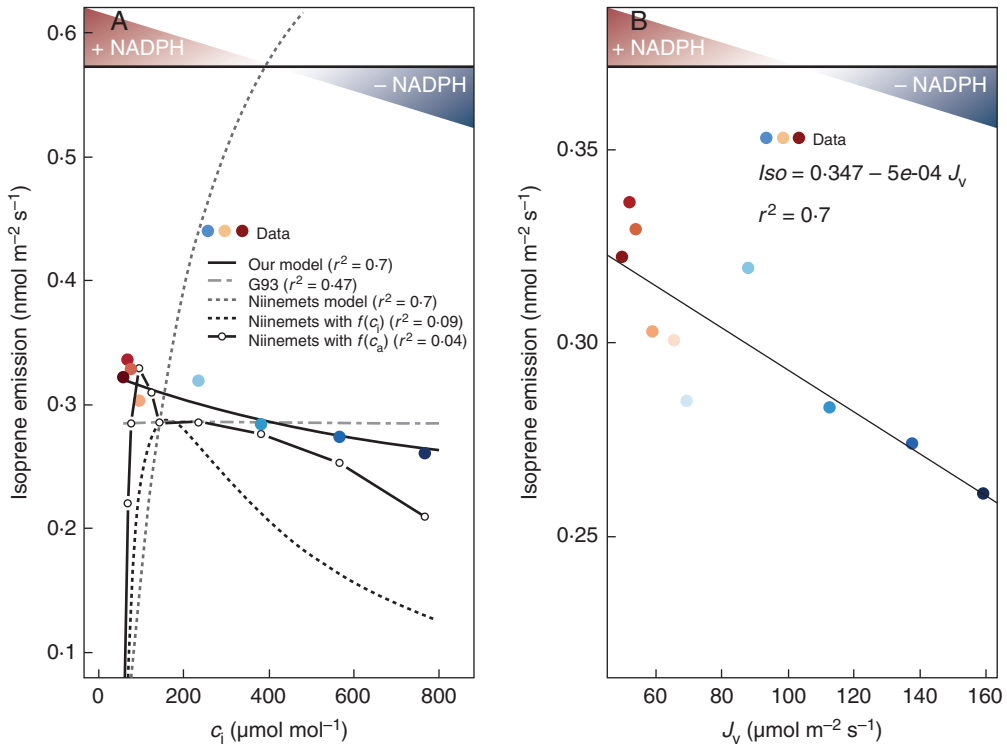

FIG. 6. The relationship between isoprene emission and NADPH availability for carbon assimilation with changing internal CO_2 concentration c_i. (A) Decreasing isoprene emissions with increasing leaf-internal CO_2 concentration, c_i (data from Possell and Hewitt, 2011); $T = 30$ °C, PAR = 1000 µmol m^{-2} s^{-1}. Simulations made with our model, G93 and the Niinemets model are as indicated in the key. The dashed black line represent the Niinemets model with an additional CO_2 effect represented by $f(c_i) = c_i\ [c_a = 390$ µmol mol$^{-1}]/c_i$, where c_a is the atmospheric CO_2 concentration. The plain grey line represent the Niinemets model with an alternative additional CO_2 effect represented by $f(c_a) = [c_a = 390$ µmol mol$^{-1}]/c_a$. The terms $f(c_i)$ and $f(c_a)$ are adapted from Arneth *et al.* (2007*a*). Standard isoprene emission factor (I_s) is taken as the observed emission at $c_a = 390$ µmol mol^{-1}. (B) The linear regression between isoprene data and the electron flux required for carbon assimilation by Rubisco (J_v). Plant-specific isoprene parameters (**a**, **b**) are estimated from this linear regression and parameters for assimilation (V_{cmax}, J_{max}) were fitted to the observations by minimizing the residual sum of squares (RSS). In both panels, the availability of reducing power (NADPH) for CO_2 assimilation is represented by a colour scheme, from dark blue (deficit) to dark red (excess).

(Fig. 10A, B). This behaviour is not realistic, so the model may be overestimating the effect of $(J - J_v)$ at low PAR.

We infer that energetic control alone is insufficient to fully explain the observed temperature dependency of isoprene emission. In principle the activities of enzymes along the MEP pathway should also influence the production rate of DMADP, but very little is known about their temperature responses (Zimmer *et al.*, 2000). Temperature optima for isoprene production are shifted toward higher temperature than T_{opt_J}, probably because a decrease in DMADP pool size is compensated for by an increase in IspS activity (Rasulov *et al.*, 2010). Taking into account the temperature response of IspS, we can reproduce this shift (Figs 9C and 10C). So we suggest that temperature effects on enzyme activity may need to be considered, as well as temperature effects on electron availability.

A further limitation of our model is the paucity of available information on the temperature responses of J_{max} and V_{cmax} (Medlyn *et al.*, 2002; Kattge and Knorr, 2007). The experiments needed to quantify these responses are time-consuming, and in particular, few studies have included temperatures >40 °C. In general we would expect a decline in DMADP production for temperatures >40 °C due to thylakoid damage, while at temperatures above 45–48 °C irreversible damage to enzyme function will cause isoprene emission to cease.

Using data from Medlyn *et al.* (2000) and references therein, we checked variations with temperature of electron availability among isoprene emitting species at 1000 µmol m^{-2} s^{-1} PAR (Fig. 11). We also tested the influence of the temperature response parameterization of V_{cmax} by contrasting an Arrhenius function with a peak function (Supplementary Data), as described in Medlyn *et al.* (2000). The temperature optima for the selected species are all higher for V_{cmax} than J_{max} (Medlyn *et al.*, 2002; Kattge and Knorr, 2007). Consequently, we predicted a decline in DMADP pool size above T_{opt_J}, due to the decline of J being accompanied by a decline in $(J - J_v)$, but the shape of the decline depended on the parameterization adopted.

DISCUSSION

We have used a conceptual model to ask whether variation in the availability of NADPH in the chloroplast can plausibly account for observed changes in isoprene emission with PAR, c_i and leaf temperature. The answer is yes. By modelling isoprene emission as proportional to a simple metric of the excess or deficit of electrons relative to the demands of carbon assimilation, we have provided a unifying explanation for the lack of close coupling of isoprene emission with carbon assimilation, the disparities in

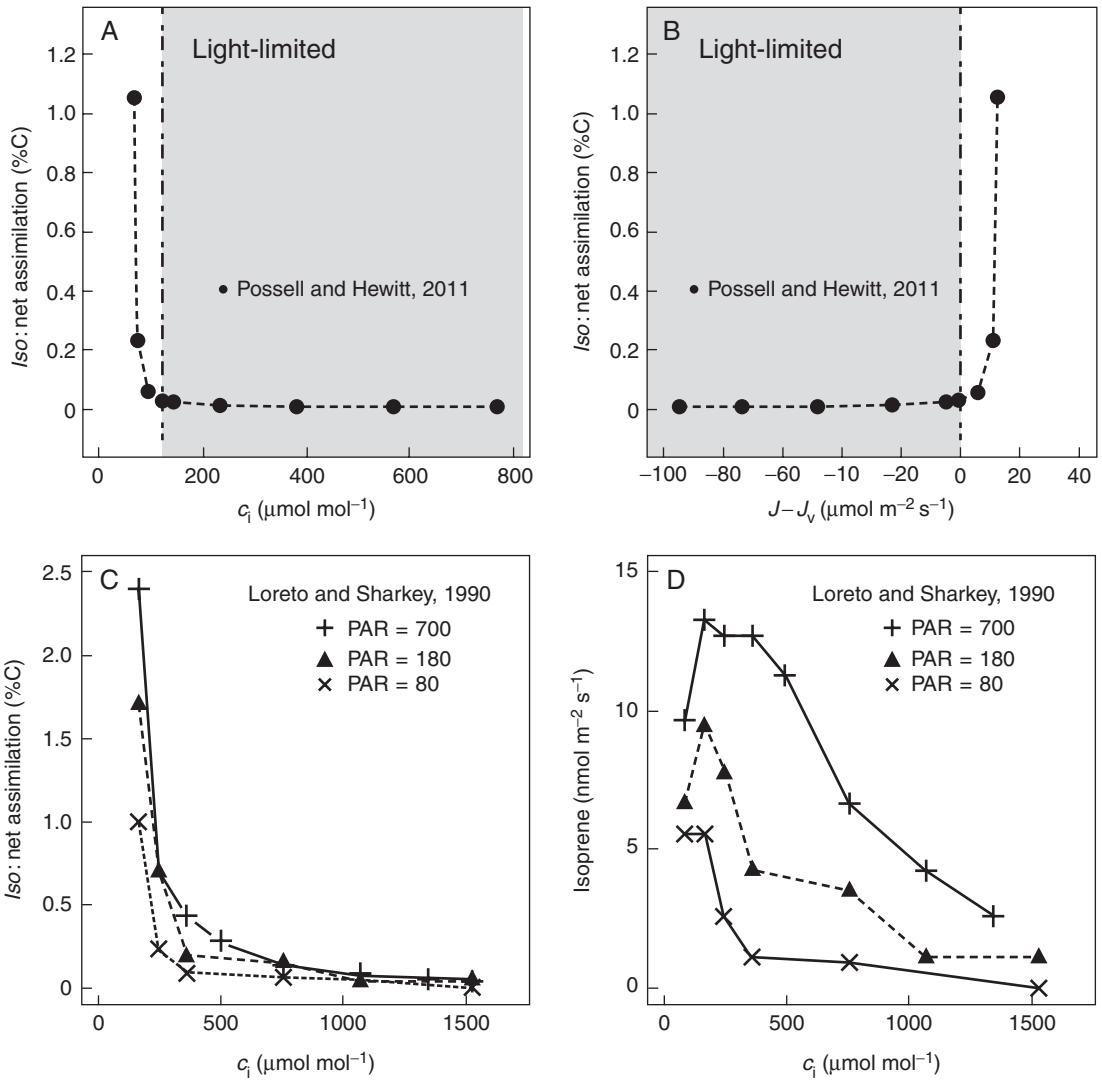

FIG. 7. Observed changes in the ratio of isoprene emission to net carbon assimilation with changes in (A) leaf-internal CO_2 concentration (c_i), (B) electron excess ($J - J_v$) (data from Possell and Hewitt, 2011). Observed changes with c_i of (C) the ratio of isoprene emission to carbon assimilation and (D) isoprene emission, for three PAR fluxes (μmol m^{-2} s^{-1}). Data digitized from Loreto and Sharkey (1990).

carbon allocated to isoprene production, high isoprene emissions at low c_i and the shift of the temperature optimum for isoprene emission above that of carbon assimilation but below that of isoprene synthase.

To our knowledge, this is the first study that has attempted to model the flux of reducing power into the MEP production pathway based on the idea of a balance between electron supply and demand. Our hypothesis invokes mechanisms that are incompletely understood and thus is to some extent speculative. Nevertheless, it appears to have significant predictive power in explaining the already documented responses of isoprene emission to PAR, c_i and (with some caveats) temperature. Moreover, this hypothesis provides a parsimonious explanation for the response of isoprene emission to drought. Under moderate to mild drought where the photosynthetic apparatus is not damaged (Cornic and Briantais, 1991), carbon assimilation is first reduced by stomatal closure (and thus reduced c_i). Under higher drought severity, this reduction is greatly increased by decreased ATP in water-deficient leaves (Lawlor and Tezara, 2009), which reduces the photosynthetic metabolic potential (A_{pot}), even if c_i increases due to light respiration. The resulting oversupply of reducing power ensures that isoprene emissions continue at a high rate, although carbon assimilation is reduced (Niinemets, 2010). However, a decrease in ATP could also reduce isoprene emissions. Under extreme drought, however, damage to the photosynthesis apparatus eventually results in the cessation of both carbon assimilation and isoprene emission.

A strong diurnal cycle is observed in isoprene emission at canopy scales. Low emissions during early morning and late afternoon contrast with high emissions during the midday period (Hewitt *et al.*, 2011; Keenan and Niinemets, 2012). Our hypothesis explains this as a consequence of higher PAR and temperature, and lower c_i due to partial stomatal closure associated with higher evaporative demand in the midday period. This simple explanation does not require the intervention of a circadian clock, as had been proposed by Hewitt *et al.* (2011).

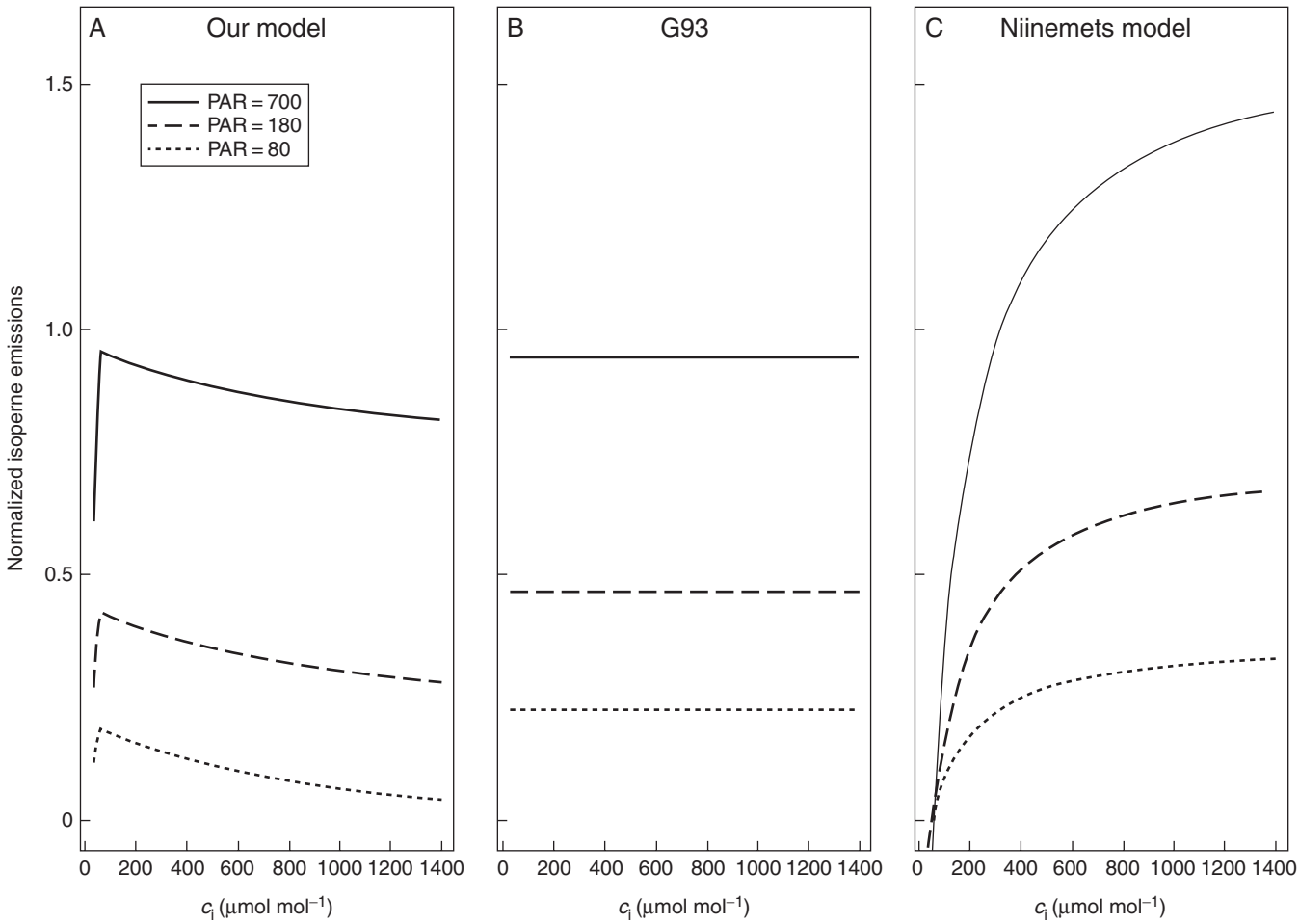

FIG. 8. Modelled responses of isoprene emission versus c_i for three PAR fluxes (80, 180 and 700 μmol m^{-2} s^{-1}). (A) our model, (B) G93 and (C) the Niinemets model. Parameters values as in Fig. 2. Emissions were normalized to a standard emission rate at $T = 30$ °C, $c_i = 273$ μmol mol^{-1}, PAR = 1000 μmol m^{-2} s^{-1}.

Note that we are *not* advocating a function of isoprene emissions as an 'electron sink' as was earlier proposed (e.g. Logan *et al.*, 2000). It is clear from the findings of Li and Sharkey (2012) that the quantity of electrons used in isoprene synthesis is far too small for this function to be plausible. The low affinity of IspS for DMADP already argues strongly against this notion (Silver and Fall, 1995; Schnitzler *et al.*, 1997). Our model implies that the allocation of reducing power to this pathway occurs under those conditions when electron availability is in excess, which fortuitously occurs during stress events when isoprene biosynthesis and emission is advantageous to the plant (e.g. Sharkey *et al.*, 2001; Vickers *et al.*, 2009).

Our results provide an alternative, robust approach to modelling isoprene emissions for global change applications. But more work is needed before implementing the model in a global context. Particular attention should be given to the influence of enzymatic activity on temperature responses of the modelled rates of isoprene. The values of the parameters **a** and **b** (eqn 1), and their potential species and environmental dependencies, also call for further investigation at several scales:

(1) For leaves, by setting up experiments that could test interactions among the short-term responses of isoprene emission to different environmental drivers, and associated variations in the excess of electrons (i.e. isoprene/assimilation responses to c_i at different PAR fluxes, together with isoprene/assimilation response to PAR at different c_i); and the influence of growth conditions on the parameters. Note that, as most of the process-based models are closely linked to photosynthesis models, information on the values of V_{cmax} and J_{max} associated with the isoprene standard emission rate would be valuable.

(2) For ecosystems, by upscaling the model from the leaf scale to the canopy, with particular attention to the response of Iso/A_{gross}. This step would require a representation of the canopy structure and vertical mixing as well as the canopy chemistry accounting for isoprene oxidation, deposition and OH regeneration.

(3) At the global scale, with the possibility of using remotely sensed formaldehyde column concentrations to better constrain model parameters for different plant function types and environments. Formaldehyde is a product of isoprene oxidation. As it is observed by satellite, with global coverage, numerous studies have used formaldehyde data to investigate isoprene emission at larger scales (Palmer *et al.*, 2003, 2006; Barkley *et al.*, 2008; Stavrakou *et al.*, 2009; Fortems-Cheiney *et al.*, 2012).

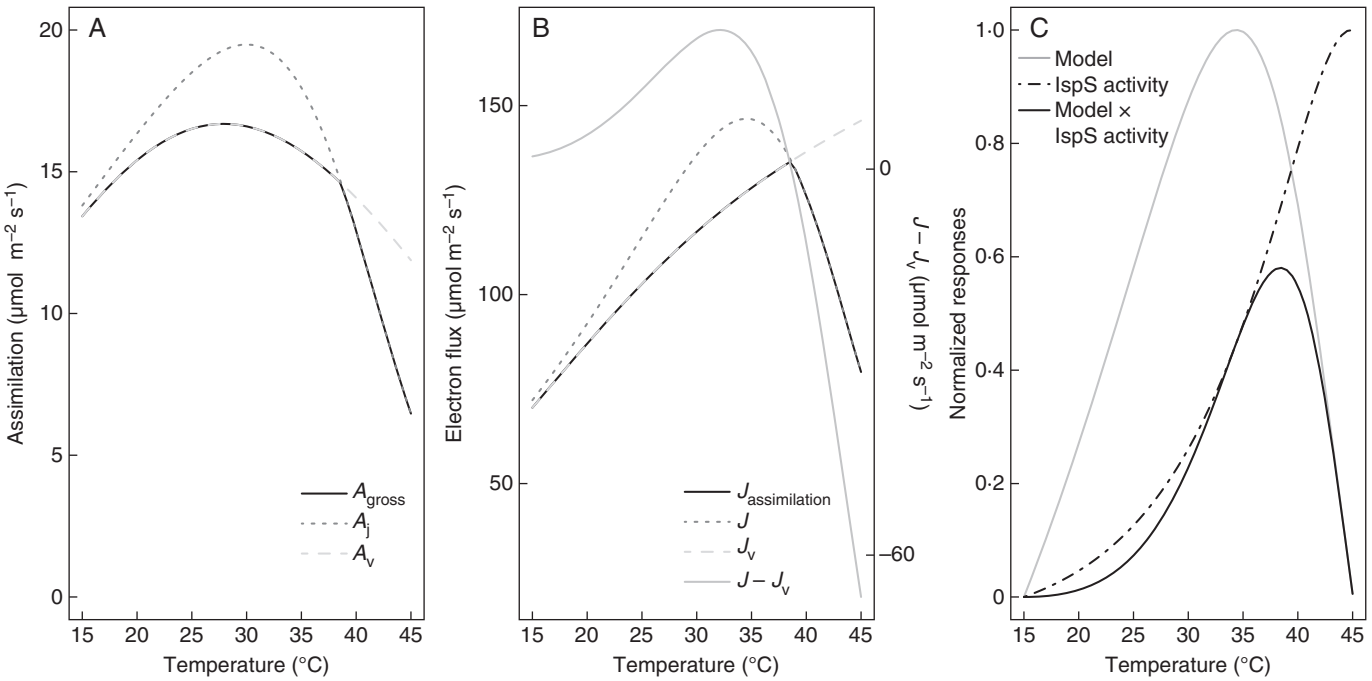

FIG. 9. Explanation of the predicted temperature dependency of isoprene emissions. (A) The responses to temperature of the light-limited A_j, the Rubisco-limited A_v and the gross assimilation A_{gross} (as indicated in key); (B) the associated electrons fluxes (left-hand axis) and the associated electron availability ($J - J_v$) (right hand axis). (C) The normalized responses to temperature of our model, normalized IspS activity and the resulting product (see key). Temperature dependency of IspS is as described in Niinemets *et al.* (1999). Parameters values of the model are taken as in Fig. 2.

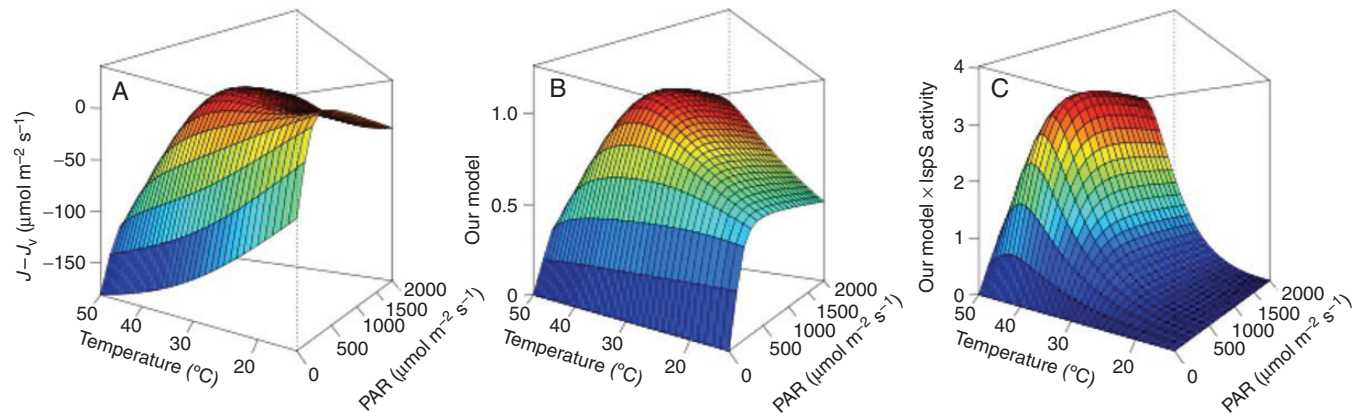

FIG. 10. Responses to variation in temperature (°C) and PAR (μmol m^{-2} s^{-1}) of electron availability ($J - J_v$) (μmol m^{-2} s^{-1}) (A), our model (B) and our model simulations multiplied by a normalized function of enzymatic activity (C). Farquhar model parameters are for *Quercus robur*, as described in Medlyn *et al.* (2002). Isoprene model parameters **a** and **b** (eqn 1) are based on data of Possell and Hewitt (2011) (fig. 6). Model outputs in A and C are normalized to be unity at $T = 30$ °C and PAR = 1000 μmol m^{-2} s^{-1}.

A comprehensive approach to isoprene modelling would also have to account for longer-term acclimation over a time scale of weeks to months, including responses to antecedent temperatures (Guenther *et al.*, 2006), phenological stages, and differences between the short-term and acclimated responses to CO_2 (Sun *et al.*, 2012), which are presumably mediated by transcriptional control of the MEP pathway enzymes. It would be of particular interest to examine whether these acclimatory changes in isoprene emission are correlated with acclimatory changes in reducing power. However, some acclimatory shifts are unlikely to be explained by a model based on reducing power alone. For example, growth at higher temperatures leads to increased emission rates measured at a common temperature (Pétron *et al.*, 2001; Niinemets *et al.*, 2010), whereas reducing power at a given temperature tends to be reduced by high growth temperatures due to a decline in the J_{max}/V_{cmax} ratio (Hikosaka *et al.*, 1999; Onoda *et al.*, 2005). Longer-term responses of isoprene emission to changes in growth temperature are therefore

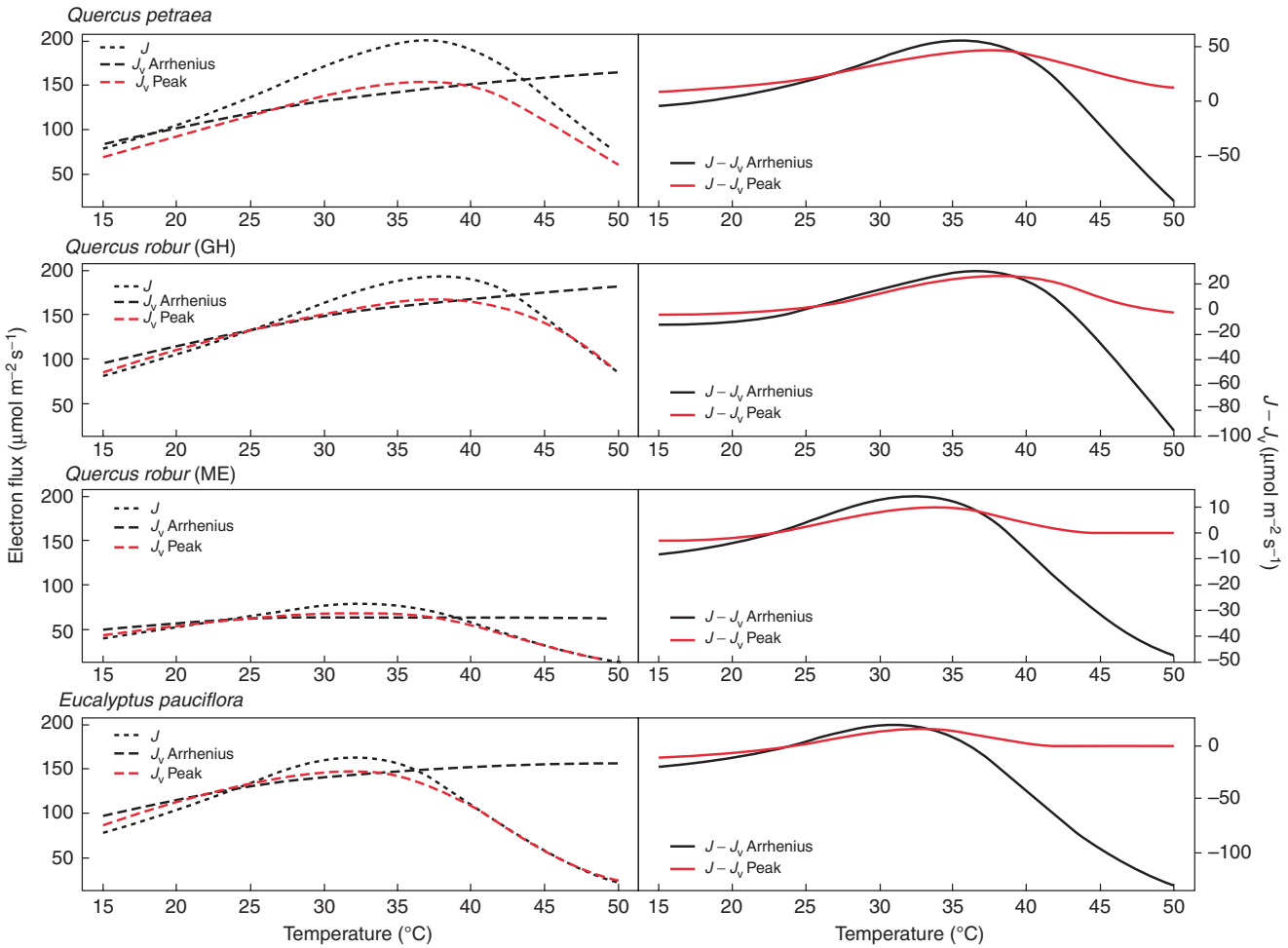

FIG. 11. Left: temperature responses for different species of the light-limited electron flux (J) (dark grey dotted line), the Rubisco-limited electron flux (J_v) using an Arrhenius function for V_{cmax} (J_v Arrhenius, black dashed line), and the Rubisco-limited electron flux using a peak function for V_{cmax} (J_v peak, red dashed line). Right: the resulting temperature responses of ($J - J_v$), using an Arrhenius function for V_{cmax} (black solid line), and a peak function for V_{cmax} (red solid line). Farquhar parameters and calculation of V_{cmax} are as described in Medlyn *et al.* (2000). For *Quercus robur*: GH, greenhouse experiment; ME, mini-ecosystem experiment (Medlyn *et al.*, 2000). Simulations are done for $c_i = 273$ μmol mol^{-1} and PAR = 1000 μmol m^{-2} s^{-1}.

presumably governed by other factors, including transcriptional control of the MEP pathway enzymes.

Conclusions

A simple model of the biochemistry and physiology of isoprene emissions has been developed and used to test the hypothesis that the reducing power available to the synthesis pathway for isoprene varies according to demands of carbon assimilation. The model explains the observed response of isoprene production to environment and the coupling/decoupling between carbon assimilation and isoprene emission. The model has the potential to improve global-scale modelling of vegetation isoprene emissions, as well as emissions of isoprenoids that do not originate from storages.

SUPPLEMENTARY DATA

Supplementary data are available online at www.aob.oxfordjournals.org and consist of details of the following. The G93 algorithm for prediction of isoprene emission from vegetation; the Niinemets model based on quantifying the NADPH cost for isoprene synthesis; and the model for photosynthetic carbon assimilation based on the Farquhar model.

ACKNOWLEDGEMENTS

We thank Karena McKinney for providing the original isoprene data for the Harvard forest site. We thank Russell Monson and Rüdiger Grote for their helpful and constructive comments on the manuscript. C.M. and I.C.P. have received funding from the European Community's Seventh Framework Programme (FP7 2007–2013) under grant agreement no. 238366.

LITERATURE CITED

Affek HP, Yakir D. 2003. Natural abundance carbon isotope composition of isoprene reflects incomplete coupling between isoprene synthesis and photosynthetic carbon flow. *Plant Physiology* **131**: 1727–1736.

Arneth A, Niinemets Ü, Pressley S, *et al*. 2007*a*. Process-based estimates of terrestrial ecosystem isoprene emissions: incorporating the effects of a direct CO_2-isoprene interaction. *Atmospheric Chemistry and Physics* **7**: 31–53.

Arneth A, Miller PA, Scholze M, *et al*. 2007*b*. CO_2 inhibition of global terrestrial isoprene emissions: potential implications for atmospheric chemistry. *Geophysical Research Letters* **34**: L18813.

Arneth A, Schurgers G, Lathiere J, *et al*. 2011. Global terrestrial isoprene emission models: sensitivity to variability in climate and vegetation. *Atmospheric Chemistry and Physics* **11**: 8037–8052.

Barkley MP, Palmer PI, Kuhn U, *et al*. 2008. Net ecosystem fluxes of isoprene over tropical South America inferred from Global Ozone Monitoring Experiment (GOME) observations of HCHO columns. *Journal of Geophysical Research* **113**: D20304.

Bryan AM, Bertman SB, Carroll MA, *et al*. 2012. In-canopy gas-phase chemistry during CABINEX 2009: sensitivity of a 1-D canopy model to vertical mixing and isoprene chemistry. *Atmospheric Chemistry and Physics* **12**: 8829–8849.

Campbell WH. 1988. Nitrate reductase and its role in nitrate assimilation in plants. *Physiologia Plantarum* **74**: 214–219.

Canvin DT, Atkins CA. 1974. Nitrate, nitrite and ammonia assimilation by leaves?: effect of light, carbon dioxide and oxygen. *Planta* **116**: 207–224.

Carlton AG, Wiedinmyer C, Kroll JH. 2009. A review of secondary organic aerosol (SOA) formation from isoprene. *Atmospheric Chemistry and Physics* **9**: 4986–5005.

Cen Y, Sage RF. 2005. The regulation of Rubisco activity in response to variation in temperature and atmospheric CO_2 partial pressure in sweet potato. *Plant Physiology* **139**: 979–990.

Charon L, Pale-grosdemange C, Rohmer M. 1999. On the reduction steps in the mevalonate independent 2-C-methyi-phritol 4-phosphate (MEP) pathway for isoprenoid biosynthesis in the bacterium *Zymomonas mobilis*. *Tetrahedron Letters* **40**: 7231–7234.

Claeys M, Graham B, Vas G, *et al*. 2004. Formation of secondary organic aerosols through photooxidation of isoprene. *Science* **303**: 1173–1176.

Crafts-Brandner SJ, Salvucci ME. 2000. Rubisco activase constrains the photosynthetic potential of leaves at high temperature and CO_2. *Proceedings of the National Academy of Sciences of the United States of America* **97**: 13430–13435.

Collins WJ, Derwent RG, Johnson CE, Stevenson DS. 2002. The oxidation of organic compounds in the troposphere and their global warming potentials. *Climatic Change* **52**: 453–479.

Collins WJ, Sitch S, Boucher O. 2010. How vegetation impacts affect climate metrics for ozone precursors. *Journal of Geophysical Research* **115**: D23308.

Cornic G, Briantais J-M. 1991. Partitioning of photosynthetic electron flow between CO_2 and O_2 reduction in a C3 leaf (*Phaseolus vulgaris* L.) at different CO_2 concentrations and during drought stress. *Planta* **183**: 178–184.

Delwiche CF, Sharkey TD. 1993. Rapid appearance of ^{13}C in biogenic isoprene when $^{13}CO_2$ is fed to intact leaves. *Plant, Cell and Environment* **16**: 587–591.

Eichelmann H, Oja V, Peterson RB, Laisk A. 2011. The rate of nitrite reduction in leaves as indicated by O_2 and CO_2 exchange during photosynthesis. *Journal of Experimental Botany* **62**: 2205–2215.

Fan J, Zhang R. 2004. Atmospheric oxidation mechanism of isoprene. *Environmental Chemistry* **1**: 140–149.

Farquhar GD, Von Caemmerer S, Berry JA. 1980. A biochemical model of photosynthetic CO_2 assimilation in leaves of C3 species. *Planta* **149**: 78–90.

Fortems-Cheiney A, Chevallier F, Pison I, *et al*. 2012. The formaldehyde budget as seen by a global-scale multi-constraint and multi-species inversion system. *Atmospheric Chemistry and Physics* **12**: 6699–6721.

Grote R. 2007. Sensitivity of volatile monoterpene emission to changes in canopy structure: a model-based exercise with a process-based emission model. *The New Phytologist* **173**: 550–561.

Grote R, Niinemets Ü. 2008. Modeling volatile isoprenoid emissions–a story with split ends. *Plant Biology* **10**: 8–28.

Guenther AB, Monson RK, Fall R. 1991. Isoprene and monoterpene emission rate variability: observations with eucalyptus and emission rate algorithm development. *Journal of Geophysical Research* **96**: 10799–10808.

Guenther AB, Zimmerman PR, Harley PC, Monson RK, Fall R. 1993. Isoprene and monoterpene emission rate variability: model evaluations and sensitivity analyses. *Journal of Geophysical Research* **98**: 12609–12617.

Guenther AB, Hewitt CN, Erickson D, *et al*. 1995. A global model of natural volatile organic compound emissions. *Journal of Geophysical Research* **100**: 8873–8892.

Guenther AB, Karl T, Harley P, Wiedinmyer C, Palmer PI, Geron C. 2006. Estimates of global terrestrial isoprene emissions using MEGAN (Model of Emissions of Gases and Aerosols from Nature). *Atmospheric Chemistry and Physics* **6**: 3181–3210.

Harley P, Guenther AB, Zimmerman P. 1996. Effects of light, temperature and canopy position on net photosynthesis and isoprene emission from sweetgum (*Liquidambar styraciflua*) leaves. *Tree Physiology* **16**: 25–32.

Harrison SP, Morfopoulos C, Dani KGS, *et al*. 2013. Volatile isoprenoid emissions from plastid to planet. *The New Phytologist* **197**: 49–57.

Hauglustaine DA, Lathière J, Szopa S, Folberth GA. 2005. Future tropospheric ozone simulated with a climate–chemistry–biosphere model. *Geophysical Research Letters* **32**: L24807.

Heald CL, Henze DK, Horowitz LW, *et al*. 2008. Predicted change in global secondary organic aerosol concentrations in response to future climate, emissions, and land use change. *Journal of Geophysical Research* **113**: D05211.

Heald CL, Wilkinson MJ, Monson RK, Alo CA, Wang G, Guenther A. 2009. Response of isoprene emission to ambient CO_2 changes and implications for global budgets. *Global Change Biology* **15**: 1127–1140.

Hecht S, Eisenreich W, Adam P, *et al*. 2001. Studies on the nonmevalonate pathway to terpenes: the role of the GcpE (IspG) protein. *Proceedings of the National Academy of Sciences of the United States of America* **98**: 14837–14842.

Hewitt CN, Ashworth K, Boynard A, *et al*. 2011. Ground-level ozone influenced by circadian control of isoprene emissions. *Nature Geoscience* **4**: 671–674.

Hikosaka K, Murakami A, Hirose T. 1999. Balancing carboxylation and regeneration of ribulose-1,5- bisphosphate in leaf photosynthesis: temperature acclimation of an evergreen tree, *Quercus myrsinaefolia*. *Plant, Cell and Environment* **22**: 841–849.

Karl T, Fall R, Rosenstiel TN, *et al*. 2002. On-line analysis of the $^{13}CO_2$ labeling of leaf isoprene suggests multiple subcellular origins of isoprene precursors. *Planta* **215**: 894–905.

Kattge J, Knorr W. 2007. Temperature acclimation in a biochemical model of photosynthesis: a reanalysis of data from 36 species. *Plant, Cell & Environment* **30**: 1176–1190.

Keenan TF, Niinemets Ü. 2012. Circadian control of global isoprene emissions. *Nature Geoscience* **5**: 435.

Keenan TF, Niinemets Ü, Sabate S, Gracia C, Peñuelas J. 2009. Process based inventory of isoprenoid emissions from European forests: model comparisons, current knowledge and uncertainties. *Atmospheric Chemistry and Physics* **9**: 4053–4076.

Keenan TF, Grote R, Sabaté S. 2011. Overlooking the canopy: the importance of canopy structure in scaling isoprenoid emissions from the leaf to the landscape. *Ecological Modelling* **222**: 737–747.

Kreuzwieser J, Graus M, Wisthaler A, Hansel A, Rennenberg H. 2002. Xylem-transported glucose as an additional carbon source for leaf isoprene formation in *Quercus robur*. *New Phytologist* **156**: 171–178.

Laothawornkitkul J, Taylor JE, Paul ND, Hewitt CN. 2009. Biogenic volatile organic compounds in the Earth system. *The New Phytologist* **183**: 27–51.

Lathière J, Hewitt CN, Beerling DJ. 2010. Sensitivity of isoprene emissions from the terrestrial biosphere to 20th century changes in atmospheric CO_2 concentration, climate, and land use. *Global Biogeochemical Cycles* **24**: GB1004.

Lawlor DW, Tezara W. 2009. Causes of decreased photosynthetic rate and metabolic capacity in water-deficient leaf cells: a critical evaluation of mechanisms and integration of processes. *Annals of Botany* **103**: 561–579.

Lehning A, Zimmer W, Steinbrecher R, Brüggemann N, Schnitzler J-P. 1999. Isoprene synthase activity and its relation to isoprene emission in *Quercus robur* L. leaves. *Plant, Cell and Environment* **22**: 495–504.

Lerdau MT, Keller M. 1997. Controls on isoprene emission from trees in a subtropical dry forest. *Plant, Cell and Environment* **20**: 569–578.

Lerdau MT, Throop HL. 1999. Isoprene emission and photosynthesis in a tropical forest canopy: implications for model development. *Ecological Applications* **9**: 1109–1117.

Li Z, Sharkey TD. 2012. Metabolic profiling of the methylerythritol phosphate pathway reveals the source of post-illumination isoprene burst from leaves. *Plant, Cell & Environment* **36**: 429–437.

Lichtenthaler HK. 1999. The 1-deoxy-D-xylulose-5-phosphate pathway of isoprenoid biosynthesis in plants. *Annual Review of Plant Physiology and Plant Molecular Biology* **50**: 47–65.

Lichtenthaler HK, Schwender J, Disch A, Rohmer M. 1997. Biosynthesis of isoprenoids in higher plant chloroplasts proceeds via a mevalonate-independent pathway. *FEBS Letters* **400**: 271–274.

Logan BA, Monson RK, Potosnak MJ. 2000. Biochemistry and physiology of foliar isoprene production. *Trends in Plant Science* **5**: 477–481.

Loreto F, Sharkey TD. 1990. A gas-exchange study of photosynthesis and isoprene emission in *Quercus rubra* L. *Planta* **182**: 523–531.

Loreto F, Sharkey TD. 1993. On the relationship between isoprene emission and photosynthetic metabolites under different environmental conditions. *Planta* **189**: 420–424.

Loreto F, Pinelli P, Brancaleoni E. 2004. ^{13}C labeling reveals chloroplastic and extrachloroplastic pools of dimethylallyl pyrophosphate and their contribution to isoprene formation. *Plant Physiology* **135**: 1903–1907.

Martin M, Stirling CM, Humphries SW, Long SP. 2000. A process-based model to predict the effects of climatic change on leaf isoprene emission rates. *Ecological Modelling* **131**: 161–174.

McKinney KA, Lee BH, Vasta A, Pho TV, Munger JW. 2011. Emissions of isoprenoids and oxygenated biogenic volatile organic compounds from a New England mixed forest. *Atmospheric Chemistry and Physics* **11**: 4807–4831.

Medlyn BE, Dreyer E, Ellsworth D, *et al*. 2002. Temperature response of parameters of a biochemically based model of photosynthesis. II. A review of experimental data. *Plant, Cell and Environment* **25**: 1167–1179.

Monson RK, Fall R. 1989. Isoprene emission from aspen leaves?: influence of environment and relation to photosynthesis and photorespiration. *Plant Physiology* **90**: 267–274.

Monson RK, Jaeger CH, Adams WW, Driggers EM, Silver GM, Fall R. 1992. Relationships among isoprene emission rate, photosynthesis, and isoprene synthase activity as influenced by temperature. *Plant Physiology* **98**: 1175–1180.

Monson RK, Grote R, Niinemets Ü, Schnitzler J-P. 2012. Modeling the isoprene emission rate from leaves. *The New Phytologist* **195**: 541–559.

Niinemets Ü. 2004. Costs of production and physiology of emission of volatile leaf isoprenoids. *Advances in Plant Physiology* **7**: 233–268.

Niinemets Ü. 2010. Mild versus severe stress and BVOCs: thresholds, priming and consequences. *Trends in Plant Science* **15**: 145–153.

Niinemets Ü, Tenhunen JD, Harley PC, Steinbrecher R. 1999. A model of isoprene emission based on energetic requirements for isoprene synthesis and leaf photosynthetic properties for *Liquidambar* and *Quercus*. *Plant, Cell and Environment* **22**: 1319–1335.

Niinemets Ü, Copolovici L, Hüve K. 2010. High within-canopy variation in isoprene emission potentials in temperate trees: Implications for predicting canopy-scale isoprene fluxes. *Journal of Geophysical Research* **115**: G04029.

Nozière B, González NJD, Borg-Karlson A-K, *et al*. 2011. Atmospheric chemistry in stereo: a new look at secondary organic aerosols from isoprene. *Geophysical Research Letters* **38**: L11807.

Onoda Y, Hikosaka K, Hirose T. 2005. The balance between RuBP carboxylation and RuBP regeneration: a mechanism underlying the interspecific variation in acclimation of photosynthesis to seasonal change in temperature. *Functional Plant Biology.* **32**: 903–910.

Pacifico F, Harrison S. P., Jones CD, Sitch S. 2009. Isoprene emissions and climate. *Atmospheric Environment* **43**: 6121–6135.

Pacifico F, Harrison SP, Jones CD, *et al*. 2011. Evaluation of a photosynthesis-based biogenic isoprene emission scheme in JULES and simulation of isoprene emissions under present-day climate conditions. *Atmospheric Chemistry and Physics* **11**: 4371–4389.

Pacifico F, Folberth GA, Jones CD, Harrison SP, Collins WJ. 2012. Sensitivity of biogenic isoprene emissions to past, present, and future environmental conditions and implications for atmospheric chemistry. *Journal of Geophysical Research* **117**: D22302.

Palmer PI, Jacob DJ, M. FA, Martin RV. 2003. Mapping isoprene emissions over North America using formaldehyde column observations from space. *Journal of Geophysical Research* **108**: 4180.

Palmer PI, Abbot DS, Fu T-M, *et al*. 2006. Quantifying the seasonal and interannual variability of North American isoprene emissions using satellite observations of the formaldehyde column. *Journal of Geophysical Research* **111**: D12315.

Pétron G, Harley P, Greenberg J, Guenther A. 2001. Seasonal temperature variations influence isoprene emission. *Geophysical Research Letters* **28**: 1707–1710.

Pike RC, Young PJ. 2009. How plants can influence tropospheric chemistry: the role of isoprene emissions from the biosphere. *Weather* **64**: 332–336.

Poisson N, Kanakidou M, Crutzen P. J. 2000. Impact of non-methane hydrocarbons on tropospheric chemistry and the oxidizing power of the global troposphere?: 3-dimensional modelling results. *Journal of Atmospheric Chemistry* **36**: 157–230.

Possell M, Hewitt CN. 2011. Isoprene emissions from plants are mediated by atmospheric CO_2 concentrations. *Global Change Biology* **17**: 1595–1610.

Rasulov B, Hüve K, Väalbe M, Laisk A, Niinemets Ü. 2009. Evidence that light, carbon dioxide, and oxygen dependencies of leaf isoprene emission are driven by energy status in hybrid aspen. *Plant Physiology* **151**: 448–460.

Rasulov B, Hüve K, Bichele I, Laisk A, Niinemets Ü. 2010. Temperature response of isoprene emission *in vivo* reflects a combined effect of substrate limitations and isoprene synthase activity: a kinetic analysis. *Plant Physiology* **154**: 1558–1570.

Rasulov B, Hüve K, Laisk A, Niinemets Ü. 2011. Induction of a longer term component of isoprene release in darkened aspen leaves: origin and regulation under different environmental conditions. *Plant Physiology* **156**: 816–831.

Rosenstiel TN, Potosnak MJ, Griffin KL, Fall R, Monson RK. 2003. Increased CO_2 uncouples growth from isoprene emission in an agriforest ecosystem. *Nature* **421**: 256–259.

Rosenstiel TN, Ebbets AL, Khatri WC, Fall R, Monson RK. 2004. Induction of poplar leaf nitrate reductase: a test of extrachloroplastic control of isoprene emission rate. *Plant Biology* **6**: 12–21.

Sanderson MG, Jones CD, Collins WJ, Johnson CE, Derwent RG. 2003. Effect of climate change on isoprene emissions and surface ozone levels. *Geophysical Research Letters* **30**: 1936.

Schnitzler J-P, Lehning A, Steinbrecher R. 1997. Seasonal pattern of isoprene synthase activity in Quercus robur leaves and its significance for modeling isoprene emission rates. *Botanica Acta* **110**: 240–243.

Seemann M, Tse Sum Bui B, Wolff M, Miginiac-Maslow M, Rohmer M. 2006. Isoprenoid biosynthesis in plant chloroplasts via the MEP pathway: direct thylakoid/ferredoxin-dependent photoreduction of GcpE/IspG. *FEBS Letters* **580**: 1547–1552.

Sharkey TD, Loreto F. 1993. Water stress, temperature, and light effects on the capacity for isoprene emission and photosynthesis of kudzu leaves. *Oecologia* **95**: 328–333.

Sharkey TD, Yeh S. 2001. Isoprene emission from plants. *Annual Review of Plant Physiology and Plant Molecular Biology* **52**: 407–436.

Sharkey TD, Singsaas EL, Vanderveer PJ, Geron C. 1996. Field measurements of isoprene emission from trees in response to temperature and light. *Tree Physiology* **16**: 649–654.

Sharkey TD, Chen X, Yeh S. 2001. Isoprene increases thermotolerance of fosmidomycin-fed leaves. *Plant Physiology* **125**: 2001–2006.

Sharkey TD, Wiberley AE, Donohue AR. 2008. Isoprene emission from plants: why and how. *Annals of Botany* **101**: 5–18.

Silver GM, Fall R. 1995. Characterization of aspen isoprene synthase, an enzyme responsible for leaf isoprene emission to the atmosphere. *The Journal of Biological Chemistry* **270**: 13010–13016.

Singarayer JS, Valdes PJ, Friedlingstein P, Nelson S, Beerling DJ. 2011. Late Holocene methane rise caused by orbitally controlled increase in tropical sources. *Nature* **470**: 82–85.

Singsaas EL, Ort DR, DeLucia EH. 2001. Variation in measured values of photosynthetic quantum yield in ecophysiological studies. *Oecologia* **128**: 15–23.

Stavrakou T, Müller J-F, De Smedt I, *et al*. 2009. Evaluating the performance of pyrogenic and biogenic emission inventories against one decade of space-based formaldehyde columns. *Atmospheric Chemistry and Physics* **9**: 1037–1060.

Sun Z, Niinemets Ü, Hüve K, *et al*. 2012. Enhanced isoprene emission capacity and altered light responsiveness in aspen grown under elevated atmospheric CO_2 concentration. *Global Change Biology* **18**: 3423–3440.

Trowbridge AM, Asensio D, Eller ASD, *et al*. 2012. Contribution of various carbon sources toward isoprene biosynthesis in poplar leaves mediated by altered atmospheric CO_2 concentrations. *PloS ONE* **7**: e32387.

Urbanski S, Barford C, Wofsy S, *et al*. 2007. Factors controlling CO_2 exchange on timescales from hourly to decadal at Harvard Forest. *Journal of Geophysical Research* **112**: G02020.

Valdes PJ, Beerling DJ, Johnson CE. 2005. The ice age methane budget. *Geophysical Research Letters* **32**: L02704.

Velikova V, Váarkonyi Z, Szabóo M, *et al*. 2011. Increased thermostability of thylakoid membranes in isoprene-emitting leaves probed with three biophysical techniques. *Plant Physiology* **157**: 905–916.

Velikova V, Sharkey TD, Loreto F. 2012. Stabilization of thylakoid membranes in isoprene-emitting plants reduces formation of reactive oxygen species. *Plant Signaling & Behavior* **7**: 139–141.

Vickers CE, Gershenzon J, Lerdau MT, Loreto F. 2009. A unified mechanism of action for volatile isoprenoids in plant abiotic stress. *Nature Chemical Biology* **5**: 283–291.

Vickers CE, Possell M, Hewitt CN, Mullineaux PM. 2010. Genetic structure and regulation of isoprene synthase in Poplar (*Populus* spp.). *Plant Molecular Biology* **73**: 547–558.

Wilkinson MJ, Monson RK, Trahan N, *et al*. 2009. Leaf isoprene emission rate as a function of atmospheric CO_2 concentration. *Global Change Biology* **15**: 1189–1200.

Wolfertz M, Sharkey TD, Boland W, Kühnemann F, Yeh S, Weise SE. 2003. Biochemical regulation of isoprene emission. *Plant, Cell and Environment* **26**: 1357–1364.

Young PJ, Arneth A, Schurgers G, Zeng G, Pyle JA. 2009. The CO_2 inhibition of terrestrial isoprene emission significantly affects future ozone projections. *Atmospheric Chemistry and Physics* **9**: 2793–2803.

Zimmer W, Brüggemann N, Emeis S, Giersch C, Lehning A, Steinbrecher R, Schnitzler J-P. 2000. Process-based modelling of isoprene emission by oak leaves. *Plant, Cell and Environment* **23**: 585–595.

Zimmer W, Steinbrecher R, Körner C, Schnitzler J-P. 2003. The process-based SIM – BIM model?: towards more realistic prediction of isoprene emissions from adult Quercus petraea forest trees. *Atmospheric Environment* **37**: 1665–1671.